

# Hybrid binomial Langevin-multiple mapping conditioning modeling of a reacting mixing layer

Andrew P. Wandel and R. Peter Lindstedt<sup>a)</sup>

*Department of Mechanical Engineering, Imperial College of Science, Technology and Medicine,  
Exhibition Road, London SW7 2BX, United Kingdom*

(Received 11 June 2008; accepted 4 November 2008; published online 13 January 2009)

A novel, stochastic, hybrid binomial Langevin-multiple mapping conditioning (MMC) model—that utilizes the strengths of each component—has been developed for inhomogeneous flows. The implementation has the advantage of naturally incorporating velocity-scalar interactions through the binomial Langevin model and using this joint probability density function (PDF) to define a reference variable for the MMC part of the model. The approach has the advantage that the difficulties encountered with the binomial Langevin model in modeling scalars with nonelementary bounds are removed. The formulation of the closure leads to locality in scalar space and permits the use of simple approaches (e.g., the modified Curl's model) for transport in the reference space. The overall closure was evaluated through application to a chemically reacting mixing layer. The results show encouraging comparisons with experimental data for the first two moments of the PDF and plausible results for higher moments at a relatively modest computational cost. © 2009 American Institute of Physics. [DOI: 10.1063/1.3041716]

## I. INTRODUCTION

The challenge of modeling flows with substantial finite-rate chemistry effects (e.g., extinction/reignition phenomena) has attracted recent attention<sup>1,2</sup> because modern combustion systems tend to operate closer to combustion limits to reduce emissions. The complex behavior that results from the presence of such effects cannot be accounted for by using simple models and, typically, transported probability density function (PDF)-based models are required.<sup>3</sup> Sensitivities to different closure elements, including molecular mixing,<sup>4</sup> increase during extinction and reignition processes and in the present work the prospects of combining a stochastic multiple mapping conditioning<sup>5</sup> (MMC) approach with a binomial Langevin model<sup>6</sup> for joint velocity-scalar statistics is evaluated. The current hybrid approach has the advantages of removing implementation difficulties associated with bounded scalars in the context of the binomial Langevin model, and providing simple closures for MMC coefficients (which are averages containing reference space and scalar quantities). The potential of the approach is here evaluated in the context of a chemically reacting mixing layer.

The conditional MMC approach (Ref. 5) presumes that the reference space has sufficient dimensions to completely describe the scalar fluctuations so that there are no fluctuations around the conditional means. Deterministic closures have been evaluated for homogeneous cases with multiple reference variables<sup>7-9</sup> and for inhomogeneous cases with a single reference variable.<sup>7,10</sup> However, the probabilistic MMC approach has only been implemented for homogeneous cases.<sup>7,11</sup>

In the current work, past efforts are extended by the development of a hybrid binomial Langevin-MMC model

applicable to the study of inhomogeneous flows. The binomial Langevin model<sup>6</sup> is used to solve the one-point, one-time, joint velocity-scalar PDF for the velocity and a pseudo mixture-fraction. The approach has the benefit of closing the velocity PDF and also allows velocity-scalar interactions to be incorporated naturally. Conventionally for MMC, it is necessary to calculate various coefficients (using iteration) to obtain the transport of the reference variables and then use a model to obtain the velocity conditioned on these reference variables. The inverse of this approach is used here to obtain the (single) reference variable directly from the velocity calculated by the binomial Langevin model. For the mixing of the scalars in MMC, iteration has also previously been used; by minimizing the difference between the mixture fractions obtained from the binomial Langevin model and MMC, iteration is again unnecessary and consistency between the elements of the hybrid model is sustained. The approach is evaluated by application to a mixing layer with finite-rate chemistry effects in order to assess the ability of the technique to reproduce the influence of varying Damköhler numbers (Da).

## II. THEORY

In this section, the theoretical bases for the model will be discussed in three subsections. The two component models—the binomial Langevin and MMC models—will be introduced separately and their pertinent formulae presented; finally, the procedure for constructing the hybrid model will be discussed.

### A. Binomial Langevin model

Hülek and Lindstedt<sup>12</sup> developed a generalized form of the binomial Langevin model<sup>6</sup> for the joint-PDF of velocity and multiple scalars. The formulation of the model for velocity transport (which for the current case includes the tur-

<sup>a)</sup>Author to whom correspondence should be addressed. Fax: +44 20 7589 3905. Electronic mail: p.lindstedt@imperial.ac.uk.

bulent kinetic energy dissipation rate  $\varepsilon$ , the return to isotropy of the Reynolds stresses and the dispersion in velocity space) is given below for a stochastic particle  $p$ . The stochastic differential equation for the velocity  $u_i$  is thus

$$du_i^{*p} = \frac{1}{\tau_u} (\alpha_1 \delta_{ij} + \alpha_2 \beta_{ij}) (u_j^{*p} - \langle u_j \rangle) dt + (C_0 \langle \varepsilon \rangle)^{1/2} dw_i, \quad (1)$$

where superscript “\*” represents a stochastic trajectory,  $k$  is the turbulent kinetic energy,  $\tau_u = \langle k \rangle / \langle \varepsilon \rangle$  is based on the ratio of the ensemble mean quantities,  $dw_i$  is an isotropic Wiener process and the Reynolds stress anisotropy tensor is

$$\beta_{ij} = \frac{\langle u'_i u'_j \rangle}{\langle u'_k u'_k \rangle} - \frac{\delta_{ij}}{3}. \quad (2)$$

The modeling coefficients are  $C_0=2.1$ ,  $\alpha_2=3.7$ , and  $\alpha_1 = -(\frac{1}{2} + \frac{3}{4}C_0) - \alpha_2 \beta_{ii}$ . The modeled stochastic differential equation for any scalar  $\eta$  is

$$d\eta^{*p} = \frac{G_\eta}{2\tau_\eta} (\eta^{*p} - \langle \eta \rangle) dt + (B_\eta \langle \varepsilon_\eta \rangle)^{1/2} dw_{\text{bin}}, \quad (3)$$

where  $dw_{\text{bin}}$  is a binomial Wiener process<sup>6</sup> and the mean scalar dissipation is modeled as  $\langle \varepsilon_\eta \rangle \equiv \langle \eta'^2 \rangle / \tau_\eta$  with the scalar time scale modeled as  $\tau_\eta = \frac{1}{2} \tau_u$ . This time scale approximation is likely to require modification due to the influence of chemical reaction on the time scale ratio.<sup>13,14</sup> However, extended models are currently at the tentative stage and the standard approach has been preferred. The drift and diffusion coefficients are

$$G_\eta = - \left\{ K_\eta \left[ 1 - \left\langle \left( \frac{\eta'^{(*p)}}{\eta'_*} \right)^2 \right\rangle \right] + 1 \right\}, \quad (4)$$

$$B_\eta = K_\eta \left[ 1 - \left( \frac{\eta'^{(*p)}}{\eta'_*} \right)^2 \right], \quad (5)$$

where

$$K_\eta = K_0 \left( 1 - \frac{\theta_\eta}{|\theta_\eta| + 1} \right), \quad (6)$$

$$\theta_\eta = C_K \frac{[(\eta^{*p} - \langle \eta \rangle)(u_i^{*p} - \langle u_i \rangle) - \langle \eta' u'_i \rangle] \langle \eta' u'_i \rangle}{\frac{2}{3} \langle k \rangle \langle \eta'^2 \rangle}, \quad (7)$$

with the introduced coefficients  $K_0=2.1$  and  $C_K=0.76$ . The additional definitions are

$$\eta'^{(*p)} = \eta^{*p} - \langle \eta \rangle^{*p}, \quad (8)$$

$$\eta'_* = \begin{cases} \eta'_{\text{max}}^{(*p)}, & \eta^{(*p)} > 0 \\ \eta'_{\text{min}}^{(*p)}, & \eta^{(*p)} < 0, \end{cases} \quad (9)$$

$$\langle \eta \rangle^{*p} = \eta_{\text{min}|c=c^{*p}} + (\langle \eta \rangle - \eta_{\text{min}|c=c^{*p}}) \times \frac{\eta_{\text{max}|c=c^{*p}} - \eta_{\text{min}|c=c^{*p}}}{\eta_{\text{max}|c=(c)} - \eta_{\text{min}|c=(c)}}, \quad (10)$$

where  $c$  is some basis scalar, generally the mixture fraction.

The above approach appears to account reasonably well for many of the physical processes that occur,<sup>12</sup> although difficulties arise in determining the limiting values in Eqs. (9) and (10) for reacting scalars. Hålek and Lindstedt<sup>12</sup> addressed the issue by ensuring transport along a scalar boundary. However, if the implementation is restricted to the mixture fraction alone—where the bounds are simple—then no difficulties arise.

## B. MMC model

In the MMC framework,  $n_s$  reactive scalars are solved, where  $n_s - 1$  scalars are species mass fractions  $Y_I$ , while the last is the specific enthalpy  $h$ . The deterministic form of the conditional MMC transport equation is<sup>5</sup>

$$\frac{\partial \bar{Z}_I}{\partial t} + \mathbf{U} \cdot \nabla \bar{Z}_I + A_k \frac{\partial \bar{Z}_I}{\partial \xi_k} - B_{kl} \frac{\partial^2 \bar{Z}_I}{\partial \xi_k \partial \xi_l} = W_I(\bar{\mathbf{Z}}), \quad (11)$$

where summation over repeated indices is intended,  $Z_I$  represents each scalar,  $\xi_k$  each reference variable,  $\bar{Z}_I \equiv \langle Z_I | \xi \rangle$ ,  $\mathbf{Z} \in \{Z_0, Z_1, \dots, Z_{n_s}\}$ ,  $Z_0$  is the mixture fraction,  $\mathbf{U} \equiv \langle \mathbf{v} | \xi \rangle$  is the conditional velocity,  $\mathbf{v}$  is the physical velocity,  $A_k$  is the drift coefficient,  $B_{kl}$  is the diffusion coefficient, and  $W_I$  is the source term. An advantage of MMC, as for PDF models in general, is that the source term is closed.

From the observation that the PDF of velocity is often close to Gaussian and the conventional assumption that the PDF of the reference variable is also Gaussian, the usual model for  $\mathbf{U}$  follows:<sup>5</sup>

$$\mathbf{U} = \tilde{\mathbf{v}} + \frac{\widetilde{\mathbf{v}'' Z_0''}}{\langle \xi_k Z_0 \rangle} \xi_k, \quad (12)$$

where  $\tilde{\mathbf{v}}$  is the Favre mean and  $\mathbf{v}'' = \mathbf{v} - \tilde{\mathbf{v}}$ . For  $\mathbf{U}$  to satisfy the variance of  $\mathbf{v}$ , the correlation coefficient of velocity and scalar must equal the correlation coefficient of the reference variable and scalar,

$$\frac{\widetilde{\mathbf{v}'' Z_0''}}{(\widetilde{\mathbf{v}''} \cdot \widetilde{\mathbf{v}''})^{1/2}} = \frac{\langle \xi'_k Z_0' \rangle}{(\langle \xi_k'^2 \rangle \langle Z_0'^2 \rangle)^{1/2}}, \quad (13)$$

where the fact that  $\langle \xi \rangle = 0$  has been used in defining the variances.

The stochastic form of the transport of the reference variable is<sup>5</sup>

$$d\xi_k^{*p} = A_k^0 dt + b_{kl} dw_l, \quad (14)$$

where

$$A_k^0 = - \frac{\partial B_{kl}}{\partial \xi_l} + B_{kl} \xi_l + \frac{1}{\langle \rho \rangle} \cdot \left( \langle \rho \rangle \frac{\widetilde{\mathbf{v}'' Z_0''}}{\langle \xi_k^* Z_0^* \rangle} \right) + \frac{2}{P_\xi} \frac{\partial B_{kl} P_\xi}{\partial \xi_l}, \quad (15)$$

$$2B_{kl} = b_{ki} b_{li} \quad (16)$$

and  $dw_l$  is a Wiener process. The specification of the terms in Eq. (15), particularly the third term (the inhomogeneous drift term), requires care. The formula for  $B_{kl}$  will be presented later.

With the velocity modeled using Eq. (12), it becomes a stochastic variable by virtue of  $\xi_k$  being a stochastic variable [Eq. (14)]. The physical position is then transported by the following equation:

$$d\mathbf{x}^{*p} = \mathbf{U}dt. \quad (17)$$

The flow considered here is defined by a single reactive scalar  $Y=Y_1$  and a mixture fraction  $Z=Z_0$ . Accordingly, the remaining transport equations to be solved are

$$dZ^{*p} = Sdt, \quad (18)$$

$$dY^{*p} = (S+W)dt, \quad (19)$$

where the mixing process is modeled by  $S$ . The mixing process obeys<sup>5</sup>

$$\bar{S}(\xi, \mathbf{x}, t) \equiv \langle S^{*p} | \xi^{*p} = \xi, \mathbf{x}^{*p} = \mathbf{x} \rangle \quad (20)$$

$$= 0 \quad (21)$$

so that it does not influence the (conditional) mean development of the solution.

Any model that satisfies Eq. (21) may be used for  $S$ . Due to the enforced locality of Eq. (21), models should produce improved results akin to the large eddy simulation (LES) approach by Mitarai *et al.*<sup>15</sup> In that study, results obtained with PDF models for a homogeneous domain were compared to DNS results.<sup>16</sup> The domain was then subdivided so that each cell contained a number of DNS volumes and inhomogeneous PDF modeling was performed between the LES cells. Results over the whole domain for all models tested showed a marked improvement and some models [modified Curl's and Euclidean minimal spanning tree<sup>17</sup> (EMST)] produced quantitatively similar results to the DNS. Klimenko<sup>18</sup> also discussed the effect and suggested time scales appropriate to the process and stochastic modeling approaches. Because of the improved model performance when restricted to small volumes, there is probably minimal benefit in utilizing overly complex models for  $S$ .

In LES, locality is solely defined in physical space, whereas the locality implied by Eq. (21) is partially in both physical and scalar spaces by conditioning on both. This is a feature of some turbulent combustion models—to also impose some locality in scalar space—since (after localizing the physical space) the scalar distribution is continuous in physical space (except for an initial exposure to a new stream or in the presence of shockwaves). So applying a condition such as Eq. (21) is effectively applying a refined locality in physical space—without the requirement of refining the computational grid. Refining a computational grid generally requires increasing the number of nodes in all three spatial dimensions, while Eq. (21) requires resolution of  $\xi$ -space. For a deterministic method, this generally implies at least 20 nodes per reference variable. For a fully stochastic method, if the number of reference variables is low, then no additional stochastic particles are required since sufficient numbers should be chosen to resolve the velocity PDF, although the sensitivity of scalar space and velocity space to the number of particles may be different.

In light of the above comments, the modified Curl's model<sup>19,20</sup> was applied for  $S$  and pairs of particles selected so that they are close in reference space according to

$$|\Delta \xi^{*pq}| \leq (B\Delta t)^{1/2}, \quad (22)$$

where  $\Delta \xi^{*pq}$  represents the difference in  $\xi$  between particles  $p$  and  $q$ . This process mimics the diffusive term of a stochastic differential equation [e.g., Eq. (3)], where the average distance particles diffuse is of the order of  $(B\Delta t)^{1/2}$  and the particles interact at the new location. To reduce the chances of Eq. (22) being violated,  $p$  is selected so that  $|\xi^{*p}|$  is in descending order. If no  $q$  can be found to satisfy Eq. (22), then  $q$  is selected to minimize  $|\Delta \xi^{*pq}|$ ; any violation will occur for outliers, which are in the low-probability region. If  $\Delta t$  or the number of particles is insufficient, then the model fails (which will be obvious when eventually  $\langle Z'^2 \rangle$  does not decay in the mixing substep). The conventional model for  $B$  is used,

$$B = \frac{\langle \varepsilon_{\eta} \rangle}{2} \left\langle \left( \frac{\partial Z}{\partial \xi} \right)^2 \right\rangle^{-1}, \quad (23)$$

and the derivative may require modeling. If the conditional fluctuations  $Z^{*p} - \langle Z | \xi^{*p} \rangle$  are large, then  $\partial Z / \partial \xi$  is undefined and instead  $\partial \langle Z | \xi \rangle / \partial \xi$  should be used in Eq. (23). This has been successfully used<sup>11</sup> in a homogeneous case where  $\langle Z | \xi \rangle$  was calculated using the mapping closure results,<sup>21</sup> however, the mapping closure<sup>22,21</sup> is not consistent with inhomogeneous flows and some correction is generally needed in that case.

### C. Hybrid model

Following the description of the two component models, their combination into the hybrid model will now be presented. The construction of this stochastic model is such that each particle contains the information required for both binomial Langevin and MMC transport—the approach does not require two sets of particles. All equations presented up to this point are used for the transport of the particles—with the exception of Eq. (11) [which is the deterministic form of Eqs. (17)–(19)] and Eqs. (14)–(16) (since the transport of  $\xi^{*p}$  is not directly simulated in this hybrid model). The remaining modeling, described in this section, provides values of  $\xi^{*p}$  [Eqs. (24)–(27)], models  $B$  [Eqs. (28) and (29)] and closes the model for  $S$  [see Eq. (30)]. As is the usual practice, since the modified Curl's model was used for  $S$ , the transport for  $Z^{*p}$  and  $Y^{*p}$  was not directly via stochastic differential equations. Meanwhile,  $Wdt$  was directly integrated implicitly. The binomial Langevin component directly provides the modeling for  $\xi^{*p}$ , the MMC component directly provides the modeling for  $B$  and the closure for  $S$  is provided by interaction between the two components.

In the current work, the binomial Langevin model, given in Eqs. (1)–(10), is used to obtain the velocity and a pseudo mixture-fraction  $\eta$ . The velocity is used to define the reference variable, while the pseudo mixture-fraction is used in specifying the mixing of the reactive scalars. For the flow considered here, the scalar distribution is parabolic in one dimension, homogeneous in another and inhomogeneous in

the third, so one physical coordinate is dominant. As a consequence, only one component of the velocity (in the inhomogeneous direction:  $u_2$ ) needs to be considered. In addition, a single reference variable is considered that corresponds to the mixture fraction for a two-stream mixing problem. Instead of following the conventional modeling by solving a stochastic differential equation for  $\xi$  and then defining  $\mathbf{U}$  from  $\xi$ , the opposite is preferred. That is, a distribution for  $u_i$  has been determined via a stochastic differential equation, Eq. (1), and the reference variable is calculated based on this velocity distribution. Formally, the conditional velocity defined in Eq. (12) is set to the velocity from the solution of the binomial Langevin velocity, Eq. (1),

$$U_2 = u_2^{*p}. \quad (24)$$

Equation (24) is a necessary condition for the consistency of the hybrid method because  $U_2$  is used in Eq. (17) to transport the stochastic particles in physical space. Since a similar transport equation in physical space is implied for the binomial Langevin velocity, i.e.,

$$dx_i^{*p} = u_i^{*p} dt, \quad (25)$$

the results for Eq. (1) would be inconsistent unless Eqs. (17) and (25) are identical—the distance moved in physical space is what is implied by the velocity determined from Eq. (1). A direct consequence of this is Eq. (24).

Equations (13) and (24) are substituted into Eq. (12):

$$u_2^{*p} = \tilde{u}_2 + (\tilde{u}_2^2)^{1/2} \xi^{*p}. \quad (26)$$

Finally, this formula is rearranged to produce a model for the reference variable,

$$\xi^{*p} = \frac{u_2^{*p} - \tilde{u}_2}{(\tilde{u}_2^2)^{1/2}}. \quad (27)$$

Note that  $u_2^{*p}$  varies via a stochastic differential equation, so Eq. (27) is consistent with directly solving a stochastic differential equation for  $\xi^{*p}$  (Ref. 11) and then defining  $U$  from Eq. (12). The advantage of this indirect model for  $\xi^{*p}$ , instead of directly solving its transport equation, Eq. (14), is that the quantities required for Eq. (27) are readily available, and normally calculated as part of the solution process. By contrast, the evaluation of the coefficients in Eq. (14) is not trivial and particularly the third term on the right-hand side of Eq. (15) requires careful attention.

Models which explicitly use the physical velocity as a basis for controlling the mixing of scalars have been explored in the past. One example is that by Song,<sup>23</sup> which used a function of the velocity to determine the amount of mixing for paired particles in a modified Curl's model.<sup>19,20</sup> By contrast, in the current model the *amount* of mixing is controlled by another passive scalar and the velocity is effectively used to determine *which* particles are paired. A further example is explicit conditioning on the velocity in the interaction by exchange with the conditional mean (IECM) model.<sup>24</sup> A principal difference with the current approach is that the modified Curl's model is used for the micromixing term.

In MMC, as in the conditional moment closure (CMC),<sup>25</sup> the link between the physical velocity and the conditioning variable is explicitly included in the model [the second term of Eq. (11)]. The usual method of obtaining values for the conditional physical velocity is to define the value of the conditioning variable and use a model for the velocity [such as Eq. (12)]. In MMC, unlike CMC, the conditioning variable is not a real quantity, hence provides greater flexibility in its definition. But an implementation of MMC must satisfy the fundamental criterion that the conditional mean of a scalar with respect to its reference variable monotonically varies with the reference variable. In the current approach, a value for physical velocity is already obtained for each particle via a stochastic differential equation (using the binomial Langevin model). As a consequence, the reference variable is transported so that a specific, valid solution of its stochastic differential equation is chosen. This solution is such that the value of  $U$  [from Eq. (12)] for each particle's value of  $\xi^{*p}$  is exactly the value of  $u_2^{*p}$  [from Eq. (1)] for that particle.

In the discussion following Eq. (23), it was stated that  $\partial Z / \partial \xi$  was undefined when  $Z^{*p} - \langle Z | \xi^{*p} \rangle$  is large and that  $\partial \langle Z | \xi \rangle / \partial \xi$  may be an appropriate substitution if calculated with care. Here, this approximation is formally substituted,

$$\frac{\partial Z}{\partial \xi} \approx \frac{\partial \langle Z | \xi \rangle}{\partial \xi}, \quad (28)$$

that is,

$$B \approx \frac{\langle \varepsilon \eta \rangle}{2} \left\langle \left( \frac{\partial \langle Z | \xi \rangle}{\partial \xi} \right)^2 \right\rangle^{-1}. \quad (29)$$

In practice, the derivatives were determined by subdividing the reference space and applying linear least-squares curve fits over the particles in each cell. If there are substantial conditional fluctuations  $Z^{*p} - \langle Z | \xi^{*p} \rangle$ , then the approximation of Eq. (28) is inaccurate. However, for the current model,  $B$  is only used for the purposes of Eq. (22) [it is not required to solve  $\xi^{*p}$  in Eq. (14)]. Accordingly, any error caused by using Eq. (28) should be relatively small since the diffusion length on the right-hand side of Eq. (22) is only required to be of the order of  $(B\Delta t)^{1/2}$  in practice. This is evidenced by analysis of sample distributions (Fig. 11). The relatively large scatter of  $Z^{*p}$  around  $\langle Z | \xi^{*p} \rangle$  means that altering the size of  $|\Delta \xi^{*p,q}|$  by a substantial amount ( $\sim 0.5$ ) does not significantly change the distribution of  $Z^{*q}$  inside  $|\Delta \xi^{*p,q}|$ .

The remaining task is to close the model for  $S$  by determining the degree of mixing required. This was done by requiring all particles to mix and using a least-squares analysis to set the amount of mixing so that the following is minimized:

$$|Z^{*p} - \eta^{*p}| + |Z^{*q} - \eta^{*q}|. \quad (30)$$

The criterion was chosen since both  $Z$  and  $\eta$  represent the same physical quantity—the mixture fraction—so the correspondence should be almost exact. However, a perfect correlation is not possible: for example, if  $Z^{*p} > \eta^{*p}$ , while  $Z^{*p} < Z^{*q}$ , then Eq. (30) will diverge or remain constant since  $Z^{*p}$  can only increase (towards  $Z^{*q}$ ), but Eq. (30) requires it to decrease (towards  $\eta^{*p}$ ).

Taking the Fokker–Planck pdf for the MMC model to be the expected value of the fine-grained pdf (see Appendix H<sup>26</sup>),

$$P_{\text{FP}}^M(Z, Y, \xi, \mathbf{x}; t) = \langle \delta(Z - Z^{*p}(t)) \delta(Y - Y^{*p}(t)) \times \delta(\xi - \xi^{*p}(t)) \delta(\mathbf{x} - \mathbf{x}^{*p}(t)) \rangle, \quad (31)$$

it is possible to formulate the Fokker–Planck (direct Kolmogorov) transport equation for MMC based on Eqs. (14) and (17)–(19):

$$\frac{\partial P_{\text{FP}}^M}{\partial t} + \nabla \cdot (\mathbf{U} P_{\text{FP}}^M) + \frac{\partial A^0 P_{\text{FP}}^M}{\partial \xi} - \frac{\partial^2 B P_{\text{FP}}^M}{\partial \xi^2} + \frac{\partial S P_{\text{FP}}^M}{\partial Z} + \frac{\partial(W+S) P_{\text{FP}}^M}{\partial Y} = 0. \quad (32)$$

Using the model

$$\xi^{*p} = u_2^{*p} - \tilde{u}_2, \quad (33)$$

which produces an overall model that is mathematically equivalent to the overall model implied by Eq. (27), it is possible to obtain the Fokker–Planck pdf for the hybrid model:

$$P_{\text{FP}}^H(Z, Y, u_2, \mathbf{x}; t) = \langle \delta(Z - Z^{*p}(t)) \delta(Y - Y^{*p}(t)) \times \delta(u_2 - u_2^{*p}(t)) \delta(\mathbf{x} - \mathbf{x}^{*p}(t)) \rangle. \quad (34)$$

The Fokker–Planck equation for the hybrid model is then

$$\frac{\partial P_{\text{FP}}^H}{\partial t} + \frac{\partial u_i P_{\text{FP}}^H}{\partial x_i} + \frac{\partial A_2^u P_{\text{FP}}^H}{\partial u_2} - \frac{1}{2} \frac{\partial^2 C_0 \langle \epsilon \rangle P_{\text{FP}}^H}{\partial u_2^2} + \frac{\partial S P_{\text{FP}}^H}{\partial Z} + \frac{\partial(W+S) P_{\text{FP}}^H}{\partial Y} = 0, \quad (35)$$

where

$$A_2^u = \frac{1}{\tau_u} (\alpha_1 \delta_{2j} + \alpha_2 \beta_{2j}) (u_j^{*p} - \langle u_j \rangle). \quad (36)$$

The mixing model  $S$  used in the implementation is not easily represented in this formulation.

### III. RESULTS

The above approach was applied to model the chemically reacting scalar mixing layer behind a turbulence-generating grid investigated experimentally by Saetran *et al.*<sup>27</sup> and Bilger and co-workers.<sup>28,29</sup> In the discussion below, the streamwise direction is denoted by  $x_1$ , while the direction across the mixing layer is  $x_2$  and the origin is set as the location where the splitter plate terminates at the turbulence-generating mesh. The parameters of the flow are such that the grid spacing is  $M=320$  mm, while the mean flow velocity is 0.55 m/s (accounting for the  $\sqrt{2}$  correction<sup>29</sup>). The mixtures were dilute and featured approximately 1 ppm of the reactants with  $\text{O}_3$  in the lower and  $\text{NO}$  in the upper stream. The species have similar diffusivities and are assumed to react according to the single-step reaction

TABLE I. Parameters of the simulated cases. The superscripts for the species' mole fractions are ordered by upper then lower stream.

$X_{\text{NO}}^{(1)}$ (ppm)	$X_{\text{O}_3}^{(2)}$ (ppm)	Da
4.08	3.85	2.56
0.68	0.70	0.42



with negligible heat release due to the low concentrations. Owing to the chemistry having a single step, it can be completely described by the mixture fraction  $Z$  and a reaction progress variable

$$Y = 1 - \frac{X_{\text{NO}}}{X_{\text{NO}}^{(1)}} - \frac{X_{\text{O}_3}}{X_{\text{O}_3}^{(2)}}. \quad (38)$$

Here,  $X$  is the mole fraction of the appropriate specie and superscript numbers denote the value in the corresponding inlet stream.

The chemical time scale was of the same order as the flow time and finite-rate chemistry effect were present. The chemical source terms are

$$W_{\text{NO}} = W_{\text{O}_3} = -k X_{\text{NO}} X_{\text{O}_3}, \quad (39)$$

where the rate constant is<sup>28</sup>  $k=0.388\ 87 \times 10^6\ \text{s}^{-1}$ . Two cases with Damköhler numbers of 0.42 and 2.56 (Ref. 28) were computed as summarized in Table I. Rearranging Eq. (38), the mole fractions of the reactants can be obtained from the conserved mixture fraction ( $Z$ ) and the reaction progress variable ( $Y$ ) using Eqs. (13)–(19),<sup>12</sup>

$$\frac{X_{\text{NO}}}{X_{\text{NO}}^{(1)}} = Z - Y Z_s, \quad (40)$$

$$\frac{X_{\text{O}_3}}{X_{\text{O}_3}^{(2)}} = (1 - Z) - Y(1 - Z_s). \quad (41)$$

Here  $Z_s$  is the stoichiometric mixture fraction and the formulas for the first two central moments were recorded in Eqs. (20)–(24).<sup>12</sup> The results were reported at two locations ( $x_1/M=16$  and 21) downstream of the turbulence-generating mesh.

#### A. Comparison of results

The first parameter of the mixing layer to be examined was the rate of spread defined by the 80% width,

$$\delta_{80}(x_1) = x_2(\langle Z \rangle = 0.9) - x_2(\langle Z \rangle = 0.1). \quad (42)$$

The results were essentially identical for both cases and within the experimental scatter as shown in Fig. 1. The binomial Langevin model<sup>12</sup> predicts a slightly slower spreading rate.

The results for the mean mixture fraction are shown in Fig. 2, where it can be seen that the computed results are within the experimental scatter. The results for the binomial Langevin model<sup>12</sup> were essentially the same and are not

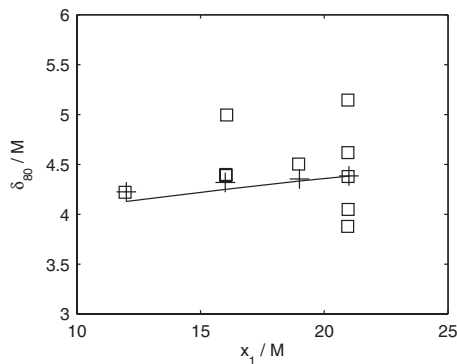


FIG. 1. Spread of mean mixture fraction profile as function of downstream location. (—) MMC; (+) binomial Langevin (Ref. 12); (□) experiment (Ref. 28).

shown for clarity. The standard deviation for the mixture fraction is shown in Fig. 3 and it can be seen that the hybrid model approximately reproduced the experimental trends. The dip in the center of the flow did not appear in the modeled results and the hybrid model underpredicted the experiment and was generally lower than for the binomial Langevin model. However, the trend for the standard deviation to increase with Damköhler number is reproduced. Bilger *et al.*<sup>28</sup> noted that all measurements were made in the initial region  $x/M < 100$ , hence the potential for variability in the statistics due to the Reynolds number and initial conditions.

The skewness (Fig. 4) and kurtosis (Fig. 5) also reproduce the overall experimental trends. The reasons for the discrepancies at the center of the flow are not clear and a more detailed analysis<sup>12</sup> suggested that experimental difficulties may be the cause. The overall trends suggest that results improved with downstream distance and as the Damköhler number was reduced. The underprediction of the standard deviation by the hybrid model is likely to be a major contributing factor to the overprediction of these higher moments. The binomial Langevin model performed well for the skewness and also predicted the kurtosis quite well for much of the range of  $x_2$ , but slightly underpredicted these moments for large  $x_2$ .

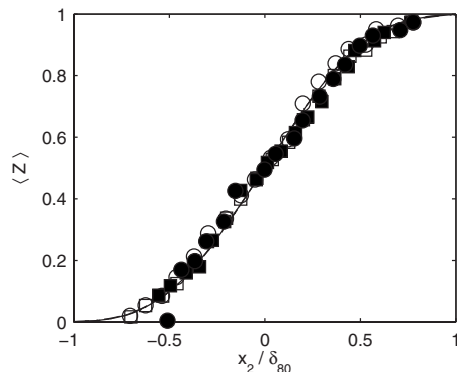


FIG. 2. Favre-averaged mixture fraction profiles. MMC: Da=2.56: (—)  $x_1/M=16$ ; (---) 21; Da=0.42: (- · - ·)  $x_1/M=16$ ; (· · ·) 21. Experiment (Ref. 28): (□)  $x_1/M=16$ ; (○) 21; Da=2.56 are the empty symbols, Da=0.42 are the filled symbols.

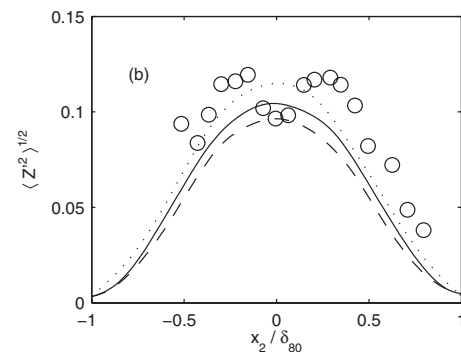
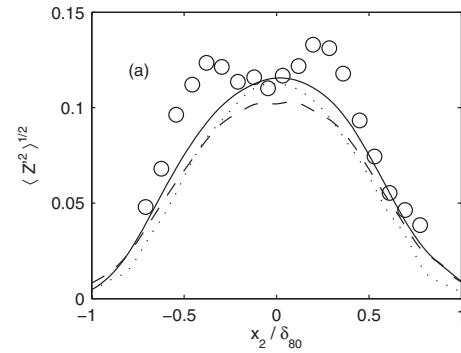


FIG. 3. Favre-averaged mixture fraction standard deviation profiles. (a) Da=2.56; (b) Da=0.42. MMC: (—)  $x_1/M=16$ ; (---) 21. Binomial Langevin (Ref. 12): (· · ·)  $x_1/M=21$ . Experiment (Ref. 28): (○)  $x_1/M=21$ .

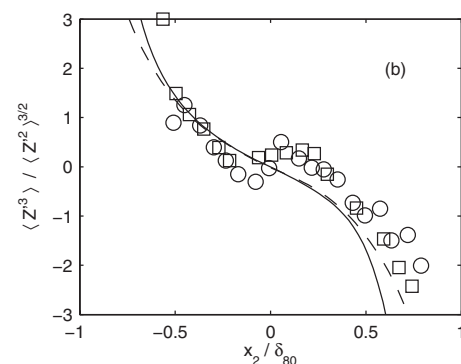
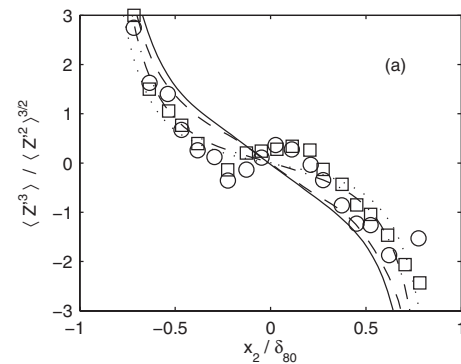


FIG. 4. Favre-averaged mixture fraction skewness profiles. (a) Da=2.56; (b) Da=0.42. MMC: (—)  $x_1/M=16$ ; (---) 21. Binomial Langevin (Ref. 12): (- · - ·)  $x_1/M=16$ ; (· · ·) 21. Experiment (Ref. 28): (□)  $x_1/M=16$ ; (○) 21.

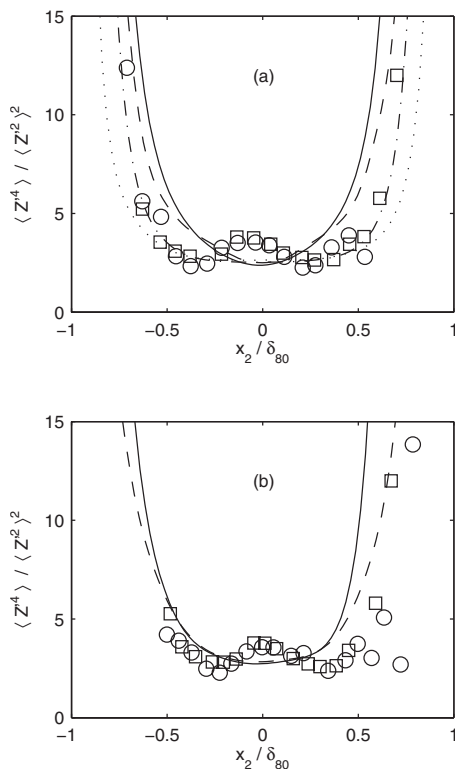
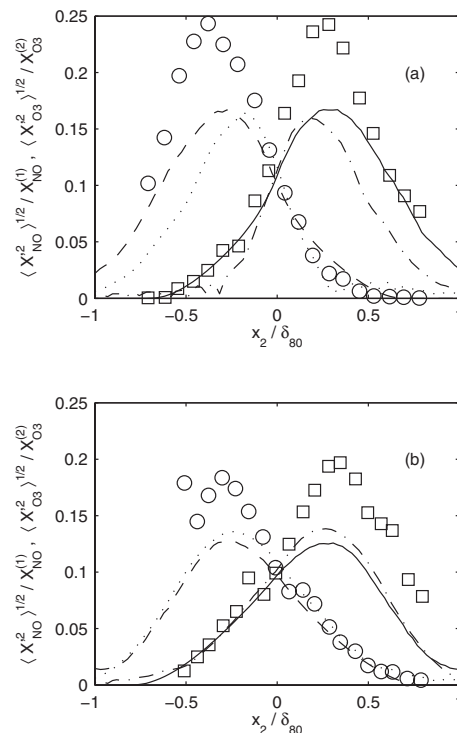
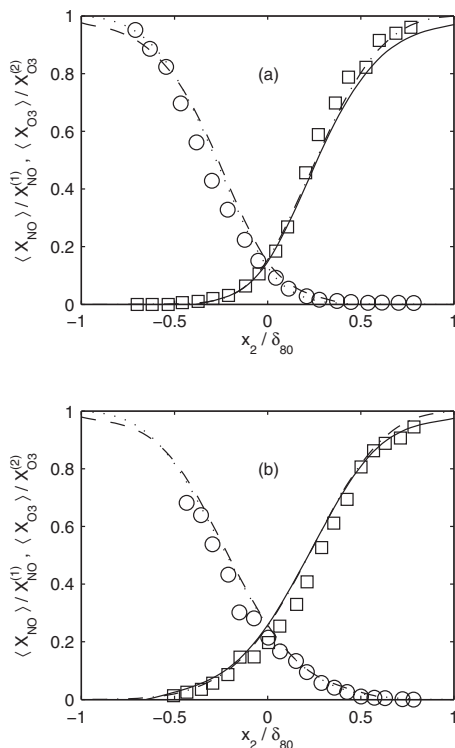


FIG. 5. Favre-averaged mixture fraction kurtosis profiles. As per Fig. 4.

FIG. 7. Favre-averaged species mole fraction standard deviation profiles at  $x_1/M=21$ . As per Fig. 6.FIG. 6. Favre-averaged species mole fraction mean profiles at  $x_1/M=21$ . (a)  $Da=2.56$ ; (b)  $Da=0.42$ . MMC: (—) NO; (---)  $O_3$ . Binomial Langevin (Ref. 12): (- · -) NO; (···)  $O_3$ . Experiment (Ref. 28): (□) NO; (○)  $O_3$ .

The mean mole fractions of the reactants are shown for  $x_1/M=21$  in Fig. 6, where it can be seen that the mean values were generally predicted quite accurately for each reactant. For the hybrid model, the large values of  $O_3$  were overpredicted; for the large values of NO, the results for  $Da=2.56$  were underpredicted and the results for  $Da=0.42$  were overpredicted. It is worth noting that where the mean mixture is stoichiometric (at  $x_2=0$ ) and the maximum reaction rate occurs, the modeled predictions were close to the experimental results. The results for the binomial Langevin model were almost identical to those for the hybrid model except for having higher values towards the freestreams.

The relative fidelity of predictions was similar for the standard deviations of the reactants (Fig. 7). Where the mean of a specie was low, the hybrid model predicted the standard deviation well, but the hybrid model underpredicted the experiment where the mean was high, although the shape was reproduced. The binomial Langevin model performed a little better than the hybrid model for  $Da=0.42$ , but was clearly worse for  $Da=2.56$ , with the peaks too narrow. The values for both models and the experiment increased with increasing Damköhler number.

The values of the covariance of the reactants are reported in Fig. 8, where it can be seen that the hybrid model results reproduced the experimental data quite well. The results for  $Da=2.56$  were narrower than those for  $Da=0.42$  in the  $x_2$ -direction for both model and experiment. The trend for the magnitude to decay with downstream distance continued, with the model producing greater maxima for  $Da=2.56$ . Indeed, the values at the center of the flow were generally well predicted, allowing for the variability of the experimental results for  $Da=0.42$  at the farthest downstream station. How-

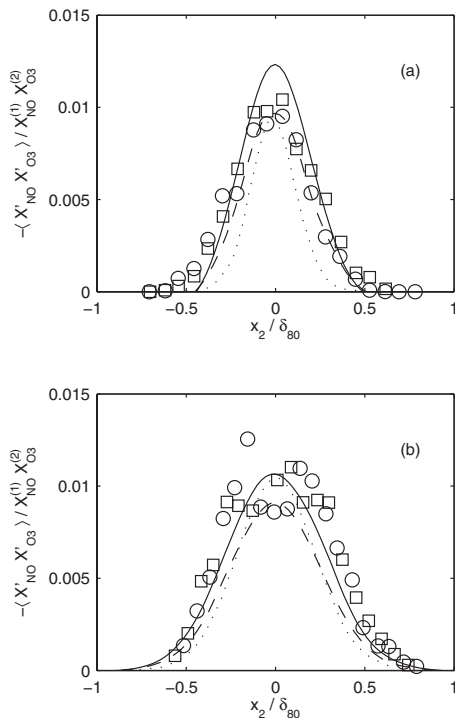


FIG. 8. Favre-averaged species mole fraction covariance profiles. (a)  $Da=2.56$ ; (b)  $Da=0.42$ . MMC: (—)  $x_1/M=16$ ; (---) 21. Binomial Langevin (Ref. 12): (···)  $x_1/M=21$ . Experiment (Ref. 28): (□)  $x_1/M=16$ ; (○) 21.

ever, the hybrid model consistently predicted that the covariance became negligible closer to the centerline than the experiment suggests. The results from the binomial Langevin model were narrower than the hybrid model, with the peaks for  $Da=2.56$  approximately the same for both models, but the binomial Langevin model produced a higher peak for  $Da=0.42$ .

The mean reaction rate across the flow is shown in Fig. 9 and it is evident that the hybrid model overpredicted the value for both Damköhler numbers. This can be contrasted with the results for the binomial Langevin model, where the mean reaction rate is consistently underpredicted. The hybrid model for  $Da=2.56$  had asymmetry to the same side as the experiment, although with a different shape; this was due to the lower mean value of NO for large  $x_2$ . The scalar PDFs for the hybrid model are shown in Fig. 10 at three cross-stream locations and a comparison with the experimental PDFs (Ref. 28) provides more information on some of the inaccuracies reported above. While the modes of the PDFs were generally correctly located (so the means were quite accurately determined)—except for the  $O_3$  side of the flow for  $Da=2.56$  [Fig. 10(d)]—the modeled PDFs were generally narrower. This caused the smaller standard deviations and larger skewness and kurtosis, discussed above.

## B. Analysis of hybrid model performance

To study the mixing process, the mixture fraction  $Z$  is plotted against its reference variable  $\xi$  and the pseudo mixture-fraction  $\eta$  in Figs. 11 and 12 respectively, while  $\eta$  is plotted against  $\xi$  in Fig. 13. Note that the last is effectively

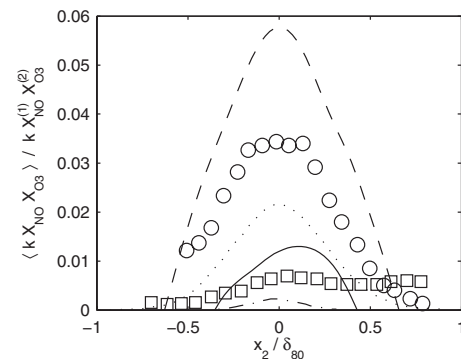


FIG. 9. Mean reaction rate profiles at  $x_1/M=21$ . MMC: (—)  $Da=2.56$ ; (---) 0.42. Binomial Langevin (Ref. 12): (---)  $Da=2.56$ ; (···) 0.42. Experiment (Ref. 28): (□)  $Da=2.56$ ; (○) 0.42.

showing the binomial Langevin model's scalar-velocity distribution. There is significant scatter evident in all figures, although both  $\langle Z|\xi \rangle$  and  $\langle Z|\eta \rangle$  show distinct trends which are generally consistent. The plots of  $Z(\xi)$  demonstrate good fidelity in probabilistic MMC modeling, while  $Z(\eta)$  show that Eq. (30) is successful in keeping  $Z$  and  $\eta$  close to each other.

Note that there were no strong correlations between  $\eta$  and  $\xi$ . Simulations which used  $\eta$  instead of  $u_2$  as the basis for  $\xi$  (using transformations in Ref. 30) produced poor results and the reasons are as follows:

- The poor correlation between  $\eta$  and  $u_2$  means that  $U_2 = \langle u_2 \rangle + (\overline{u_2'' \eta''} / \overline{\eta''^2}) \eta$  (which is a commonly used model in CMC) is not a very representative model of  $u_2(\eta)$ .
- The method used to determine the degree of mixing minimizes the difference between  $Z$  and  $\eta$ . If  $\eta$  is used as the basis for  $\xi$ , then only particles with similar  $Z$  would be allowed to mix because only particles with similar  $\eta$  would be allowed to mix [cf. Eq. (22)]. This has physical merit, reflecting the prescription of locality in MMC, and is the basis for EMST.<sup>17</sup> However, it produces “preferential mixing,” which limits the interaction of fresh mixture through turbulent fluctuations. In MMC approaches, preferential mixing limits the decay of the variance as particles repeatedly mix with the same partner. This artifact can generally be avoided by ensuring that there are sufficient particles so that (on average) more than one particle can be selected. The problem was overcome in EMST through the use of an age bias.<sup>17</sup>
- Consistency between the two components of the hybrid model is maintained by using  $u_2$  as the basis for  $\xi$ . The convective term for MMC in Eq. (11) specifies that the physical velocity is  $\mathbf{U}$ , as used in Eq. (17). By definition in the binomial Langevin model, in specifying the transport equation for the velocity  $u_i$  [Eq. (1)], this provides the physical velocity for convection [cf. Eq. (7)]. If  $\mathbf{U} \neq u_i$ , then the convection of quantities for either or both models is inconsistently represented. It is therefore necessary to use Eq. (24).

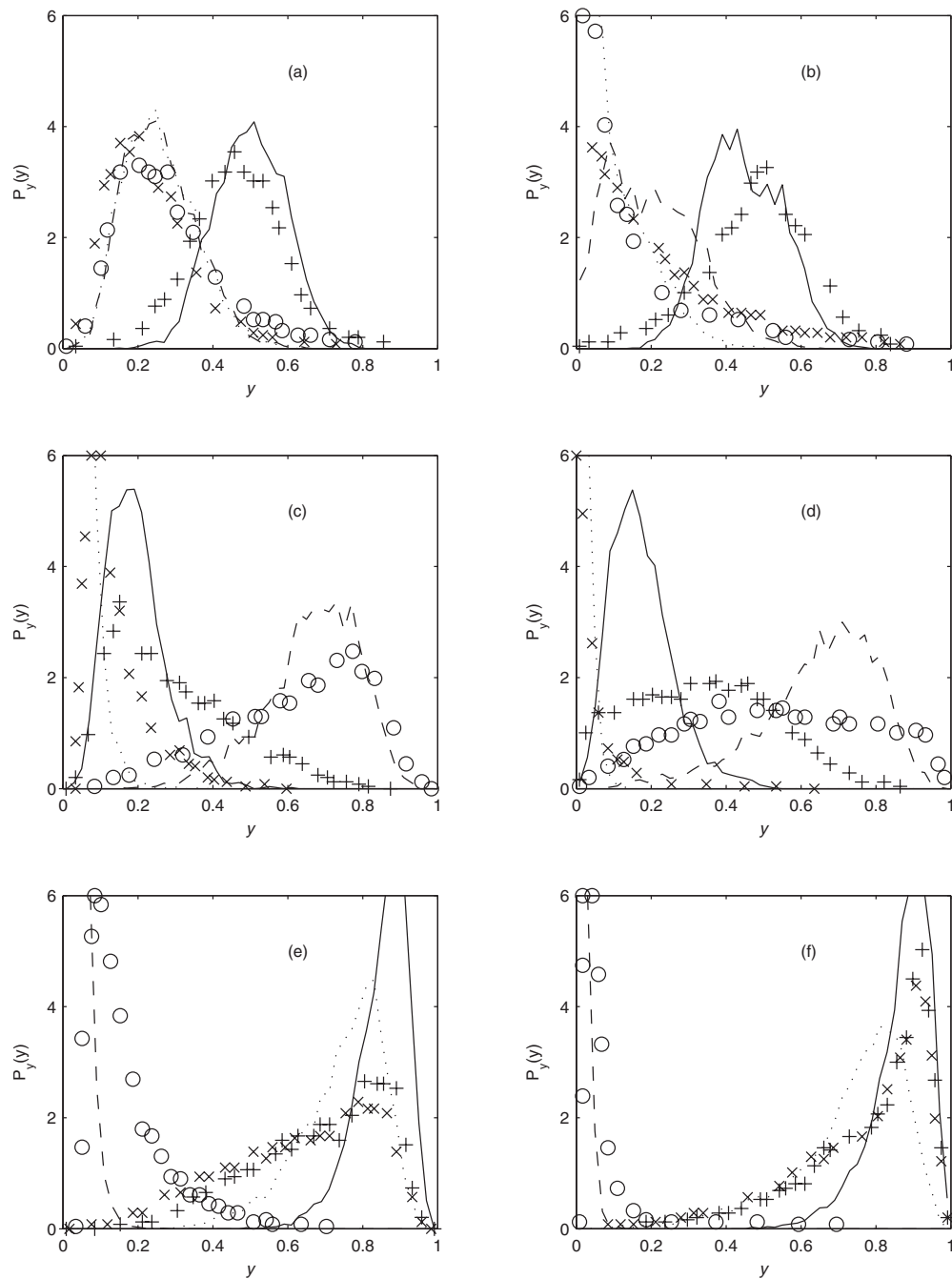


FIG. 10. PDFs at  $x_1/M=21$  for (—)  $Z$ ; (···)  $X_{NO}$ ; and (---)  $X_{O_3}$ . Experiment (Ref. 28): (+)  $Z$ ; (×)  $X_{NO}$ ; (○)  $X_{O_3}$ . Column 1:  $Da=0.42$ ; 2: 2.56. (a)  $x_2/\delta_{80}=0$ ; (b)  $-0.04$ ; (c)  $-0.36$ ; (d)  $-0.37$ ; (e)  $0.43$ ; (f)  $0.45$ .

A comparison of the covariance of the mixture fraction with its reference variable is shown in Fig. 14. The values were essentially the same for both cases, which is encouraging as the quantity appears as a parameter in the stochastic differential equation for  $\xi$  [it appears in the model for  $\mathbf{U}$ , Eq. (12)] and requires determination for a full MMC implementation. A Gaussian curve fit to the data is also shown in Fig. 14:  $c\mathcal{N}(\mu, \sigma) = -0.076\mathcal{N}(0, 0.414)$ , although the Gaussian shape is not necessarily universal.

The fact that  $\langle \xi'Z' \rangle$  is negative indicates that the profiles  $\langle Z|\xi \rangle$  resemble the *complementary* error function. Indeed, this can be seen in Fig. 11, where least-squares fits in the

form of the complementary error function are shown. Previous work on the mapping closure and MMC indicated that  $\langle Z|\xi \rangle$  should resemble the error function. Pope<sup>21</sup> showed that for the mapping closure the profiles are exactly the error function. We note that, mathematically, the complementary error function is a valid solution of the mapping closure and MMC equations because of the linearity of the equations.

Previous results for a mixing layer<sup>7</sup> produced profiles that resembled an error function. In that case, the mixture fraction in the lower stream was unity, while in the upper stream it was zero. The current situation is reversed and the effect of  $\mathbf{U} = \langle \mathbf{v}|\xi \rangle$ ,  $\partial \mathbf{U} / \partial \xi > 0$ , is to entrain material from the

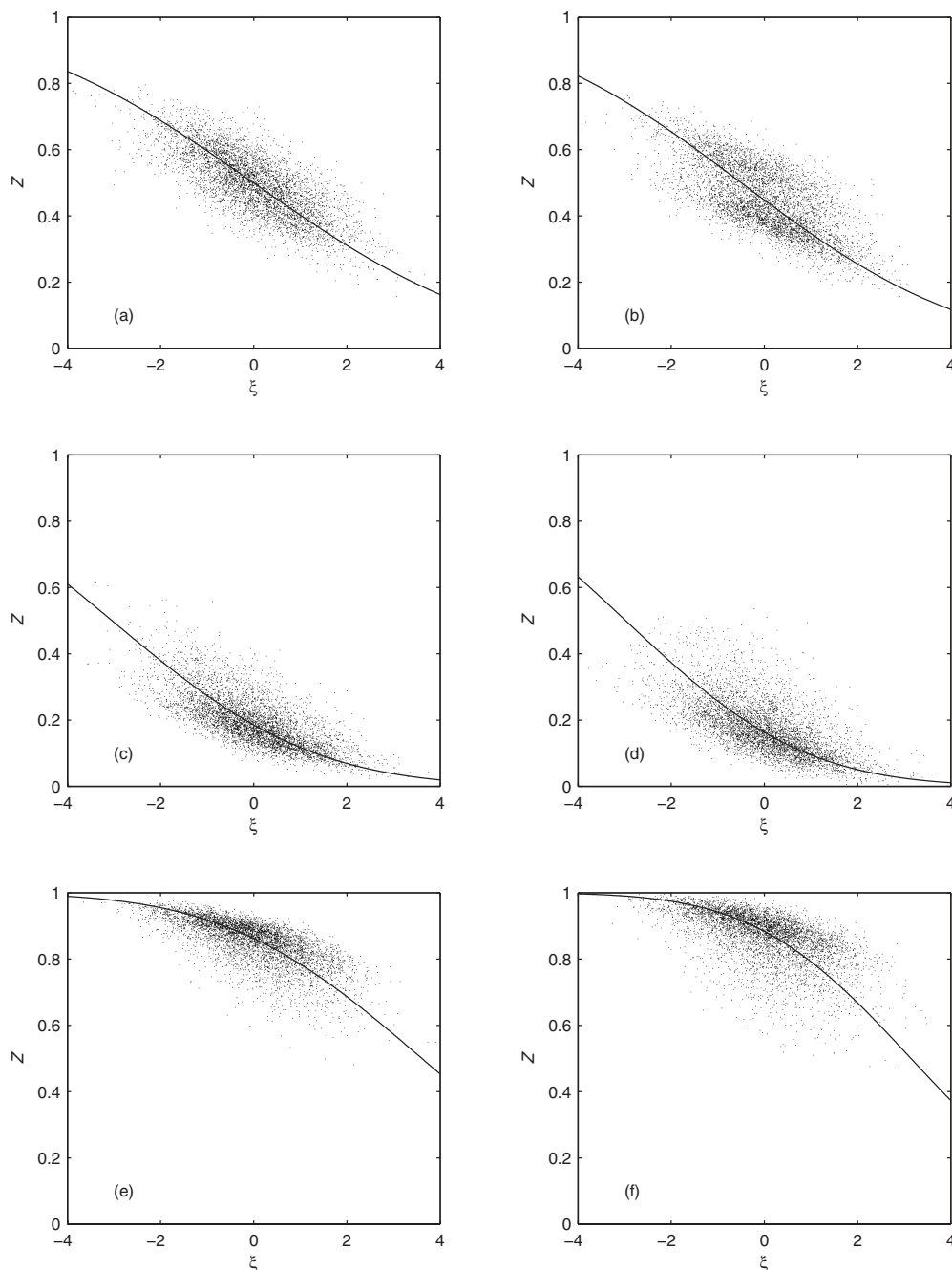


FIG. 11. Scatter plots of  $Z$  vs  $\xi$  for the same locations as Fig. 10. (—) Mapping closure solution.

unmixed streams and transport it across the flow. For the lower free stream, the mean velocity is positive, so immediately inside the mixing layer for  $\xi \geq \langle \xi \rangle$  (and for some of the range  $\xi < \langle \xi \rangle$ ),  $Z = \langle Z | \xi \rangle$  takes the value of the neighboring freestream. Based on the turbulent transport alone (considering the converse analysis of the upper freestream), the range  $\xi < \langle \xi \rangle$  is directly influenced by the upper freestream, where here  $Z$  is greater than in the lower freestream. Accordingly, the profiles of  $\langle Z | \xi \rangle$  ought to resemble the complementary error function. By reversing the coordinate direction across this mixing layer (which is possible because of the invariance of MMC to coordinate transforms), the situation would naturally be reversed and  $\langle Z | \xi \rangle$  would again resemble the

error function without any change in the statistics of the scalars. Alternatively,  $\xi$  could be defined as the negative of Eq. (27) for the same result.

The computational requirements for the hybrid model are substantially larger than for the binomial Langevin model alone, taking an order of magnitude longer on a single processor. This is due to the search for particle pairs in Eq. (22), which is not as trivial an exercise as it is for the conventional modified Curl's model, and requires approximately 90% of the computational time for the mixing substep. With the reference space being one dimensional, the particles that are physically close to each other may be sorted in reference space—a relatively fast operation—to improve the search al-

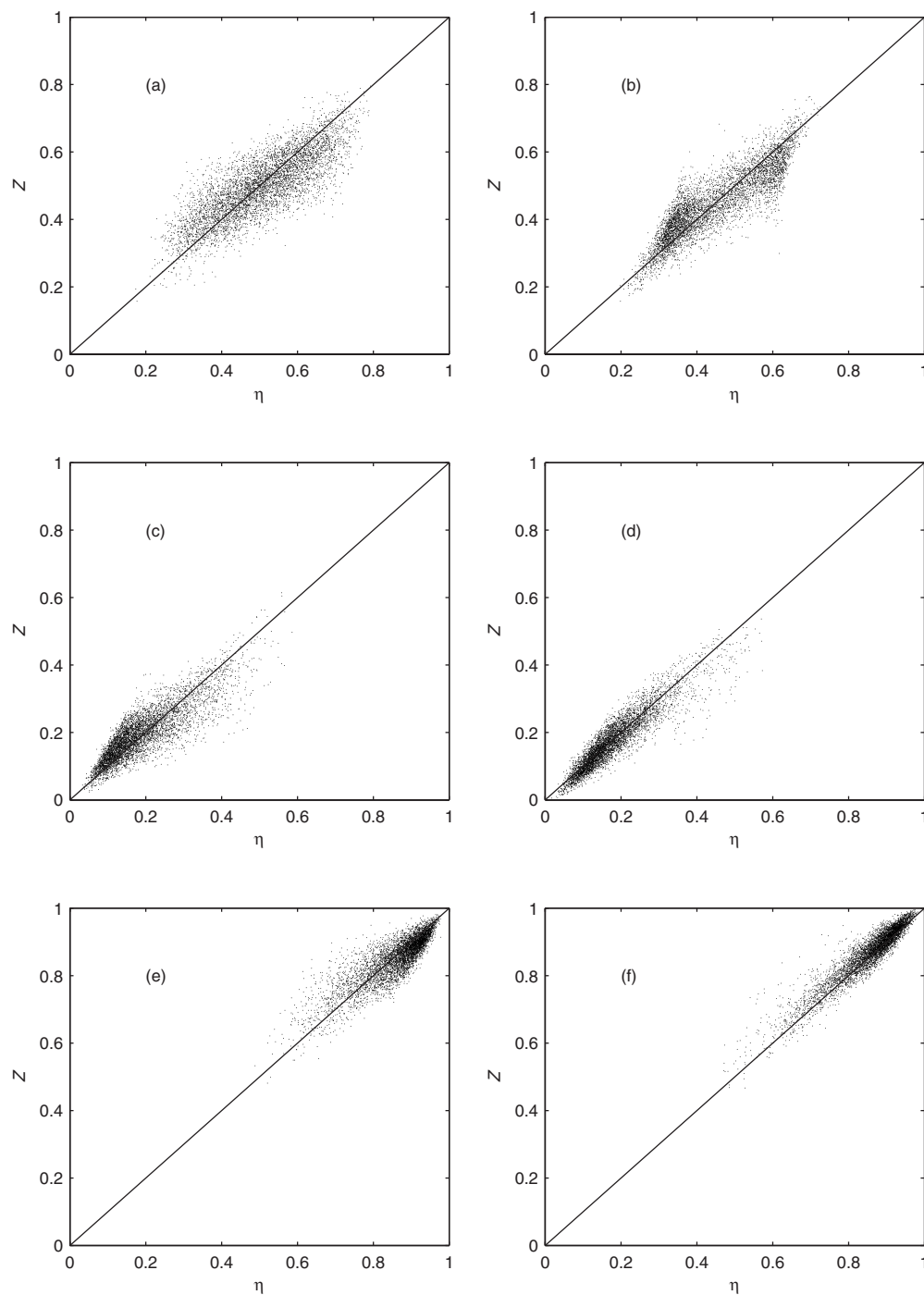


FIG. 12. Scatter plots of  $Z$  vs  $\eta$  for the same locations as Fig. 10.

gorithm, but even then the process is not trivial since adjacent particles are rarely paired. A simulation with a multidimensional reference space would be markedly slower since such a sorting procedure would be impossible. The other commonly used micromixing model which should be expected to require substantially greater computational effort than most other models is EMST. A direct comparison of computational effort between EMST and the current hybrid model has not been performed, however, it is expected that the two would require similar orders of computational effort. This is because the two models are similar in terms of finding particles that are local to other particles in composition/

reference space. For systems with a small number of variables, EMST should be quicker since the construction of the tree would be relatively straightforward and only a fraction of the particles are involved for any given computational time step. As the dimensionality of the composition space becomes large, however, and maintaining a single reference dimension for the hybrid model, EMST may become slower. Nonetheless, the single-step chemistry used for the current test case requires minimal computational effort. So when more detailed chemistry is used, which could require at least 90% of the computational effort, then the computational penalty for the particle-pairing algorithm becomes small.

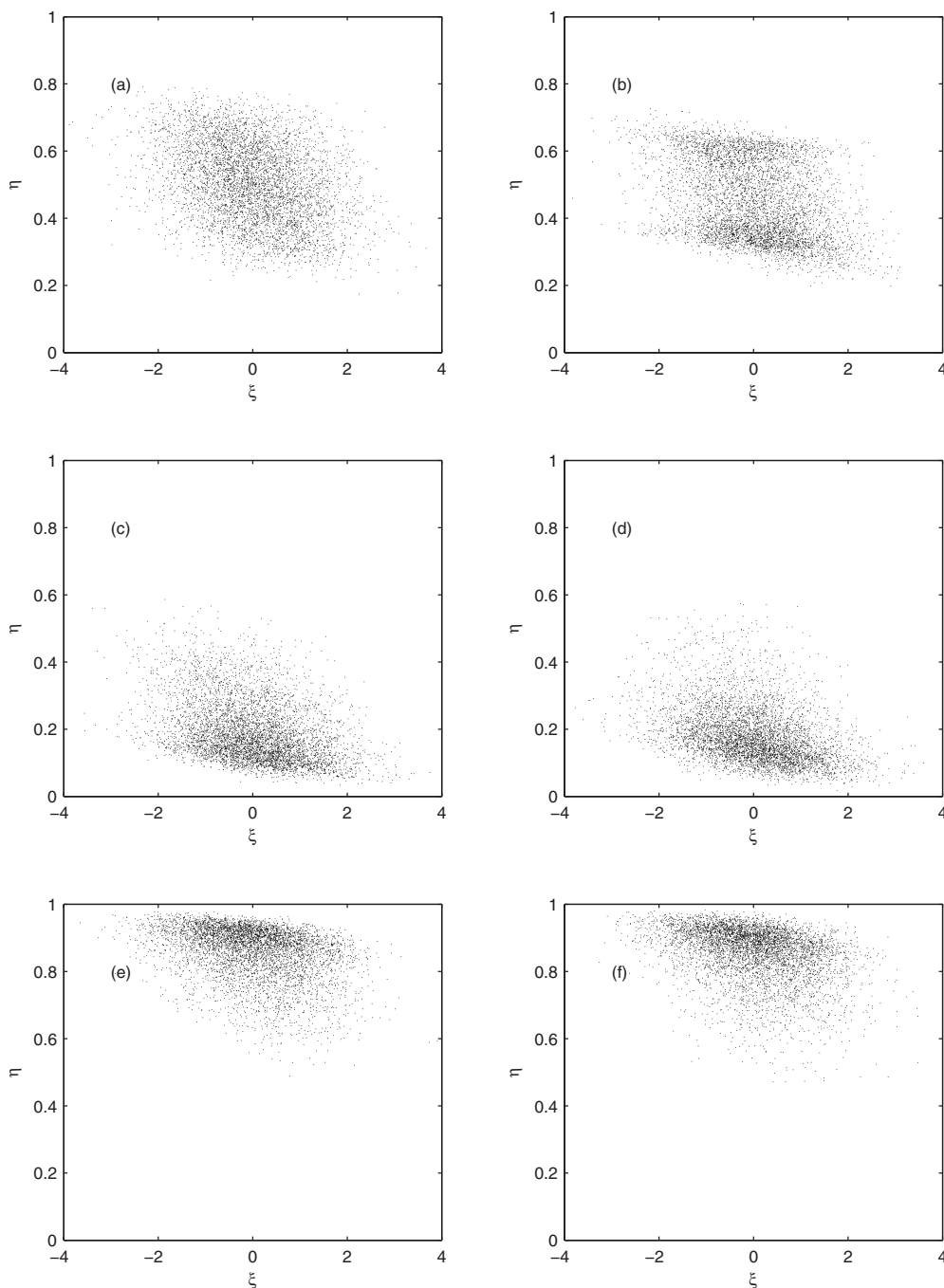


FIG. 13. Scatter plots of  $\eta$  vs  $\xi$  for the same locations as Fig. 10.

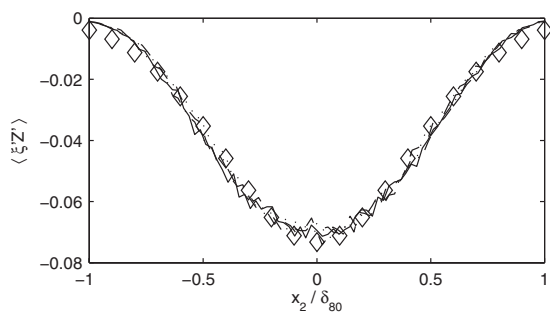


FIG. 14. Covariance  $\langle \xi'Z' \rangle$ . Lines as per Fig. 2; ( $\diamond$ ) Gaussian curve fit.

It is pertinent to compare MMC with PDF models since when the reference space has the dimensionality of the composition space, MMC becomes a PDF model, with the mapping closure concept used to close the diffusion/micromixing term. MMC has never been applied in such a way, however, since it is possible to define the system with a lower dimensionality.<sup>31</sup> When a single dimension has been used for the reference space, and this is not sufficient, a second-order closure has been used previously.<sup>7,11</sup> The two simplest PDF models, the modified Curl's model and interaction by exchange with the mean<sup>32,33</sup> are easily applied and may produce good results for simple cases, but have significant limitations in predicting higher-order moments.<sup>26</sup> There is a

similarity between MMC and EMST in that they both attempt to apply locality in composition space, however, EMST is not completely linear (it does not treat each scalar independently of all others) and it was recognized that matching particles by the smallest distance in composition space was problematic.<sup>17</sup> The relaxation of this distance was achieved in EMST via an age bias, which results in the nearest particle often being rejected (the selection chosen in Ref. 17 is that, on average, only half the particles mix in a given time step), while this relaxation is achieved in MMC via Eq. (22). Because Eq. (22) increases with  $(\Delta t)^{1/2}$ , a larger set of particles becomes available for mixing with any given particle, which is consistent with the diffusion concept. Clearly, as  $(B\Delta t)^{1/2}$  becomes small, results will become similar to EMST, while as  $(B\Delta t)^{1/2}$  becomes large, the modified Curl's model will be attained.

The major limitation for MMC is in specifying the coefficients  $\langle \xi_k^* Z_0^* \rangle$  and  $B_{kl}$ . Since these quantities involve the reference variables, standard models (such as gradient diffusion) cannot be used, since the transport coefficients are comprised of quantities which are in a mathematical space, not a physical space. The current hybrid model obtains these coefficients by relying on the one-dimensionality of the scalar field, which is clearly applicable in a free-shear flow. The broader applicability to more complex flows is yet to be determined.

#### IV. CONCLUSIONS

A hybrid binomial Langevin-MMC model has been developed and evaluated for an inhomogeneous case with finite-rate chemistry effects. This is the first effort to implement an MMC model inhomogeneously using a stochastic approach. The model is of a hybrid nature because it uses the binomial Langevin model to solve the joint velocity-scalar PDF for the velocity field and a pseudo mixture-fraction. The reference variable for the MMC model is determined directly from the velocity field to serve as a basis for the mixing of the mixture fraction and the reactive scalar. Once the mixing and chemical reaction equations have been solved, the density change is returned to the binomial Langevin model.

The simple modified Curl's model is used for the MMC mixing and was shown to work effectively when combined with the current method, which ensures proximity in scalar space of pairs of particles selected for mixing. The more complex particle-selection method is consistent with the MMC framework and does not involve much more computational expense than normally required by the modified Curl's model. An advantage of the MMC approach for the mixing process, as compared to using the binomial Langevin model for all quantities, is that the definition of scalar bounds is readily achieved within the MMC framework. The advantage of using a hybrid model for MMC is that the determination of the parameters for the transport of the reference variable are not required and that a simple approximation for the diffusion coefficient could be used as a parameter for the scalar mixing process.

The results for the mean values of the mixture fraction and mole fractions of the reactants were within experimental

error, while the general trends for the higher moments were well reproduced. The mixture fraction statistics were generally predicted better by the binomial Langevin model alone,<sup>12</sup> while some of the mole fraction statistics were predicted better by the hybrid model. The shapes of the experimental results were generally reproduced quite well by both models, although many of the second-order statistics were underpredicted.

The second-order moments are typically used as a basis for general modeling and while reasonable modeling of higher moments is naturally preferred, a lower level of accuracy is typically required. It may be concluded that the hybrid binomial Langevin-MMC model provides a reasonable level of accuracy at relatively modest computational expense and these results provide a solid basis for further testing.

#### ACKNOWLEDGMENTS

This work was funded by the EPSRC Grant No. GR/T22766 and ONR Award N000140710993. The authors also wish to thank Dr. Gabriel Roy and Dr. Andreas Kronenburg for helpful comments.

- <sup>1</sup>S. T. Smith and R. O. Fox, "A term-by-term Direct Numerical Simulation validation study of the multi-environment conditional probability-density-function model for turbulent reacting flows," *Phys. Fluids* **19**, 085102 (2007).
- <sup>2</sup>B. Merci, B. Naud, and D. Roekaerts, "Impact of turbulent flow and mean mixture fraction results on mixing model behavior in transported scalar PDF simulations of turbulent non-premixed bluff body flames," *Flow, Turbul. Combust.* **79**, 41 (2007).
- <sup>3</sup>R. P. Lindstedt, S. A. Louloudi, J. J. Driscoll, and V. Sick, "Finite rate chemistry effects in turbulent reacting flows," *Flow, Turbul. Combust.* **72**, 407 (2004).
- <sup>4</sup>Z. Ren and S. B. Pope, "An investigation of the performance of turbulent mixing models," *Combust. Flame* **136**, 208 (2004).
- <sup>5</sup>A. Y. Klimenko and S. B. Pope, "A model for turbulent reactive flows based on Multiple Mapping Conditioning," *Phys. Fluids* **15**, 1907 (2003).
- <sup>6</sup>L. Valiño and C. Dopazo, "A binomial Langevin model for turbulent mixing," *Phys. Fluids A* **3**, 3034 (1991).
- <sup>7</sup>A. P. Wandel, "Development of Multiple Mapping Conditioning (MMC) for application to turbulent combustion," Ph.D. thesis, The University of Queensland, 2005.
- <sup>8</sup>M. J. Cleary and A. Kronenburg, "Multiple mapping conditioning for extinction and reignition in turbulent diffusion flames," *Proc. Combust. Inst.* **31**, 1497 (2007).
- <sup>9</sup>M. J. Cleary and A. Kronenburg, "'Hybrid' multiple mapping conditioning on passive and reactive scalars," *Combust. Flame* **151**, 623 (2007).
- <sup>10</sup>K. Vogiatzaki, A. Kronenburg, M. J. Cleary, and J. H. Kent, "Multiple mapping conditioning of turbulent jet diffusion flames," *Proc. Combust. Inst.* **32**, 1679 (2009).
- <sup>11</sup>A. P. Wandel and A. Y. Klimenko, "Multiple mapping conditioning applied to homogeneous turbulent combustion," *Phys. Fluids* **17**, 128105 (2005).
- <sup>12</sup>T. Hülek and R. P. Lindstedt, "Joint scalar-velocity pdf modelling of finite rate chemistry in a scalar mixing layer," *Combust. Sci. Technol.* **136**, 303 (1998).
- <sup>13</sup>E. R. Hawkes, R. Sankaran, J. C. Sutherland, and J. H. Chen, "Scalar mixing in Direct Numerical Simulations of temporally evolving plane jet flames with skeletal CO/H<sup>2</sup> kinetics," *Proc. Combust. Inst.* **31**, 1633 (2007).
- <sup>14</sup>R. P. Lindstedt, H. C. Ozarovsky, R. S. Barlow, and A. N. Karpetis, "Progression of localized extinction in high Reynolds number turbulent jet flames," *Proc. Combust. Inst.* **31**, 1551 (2007).
- <sup>15</sup>S. Mitarai, J. J. Riley, and G. Kosály, "Testing of mixing models for Monte-Carlo PDF simulations," *Phys. Fluids* **17**, 047101 (2005).
- <sup>16</sup>S. Mitarai, J. J. Riley, and G. Kosály, "A Lagrangian study of scalar diffusion in isotropic turbulence with chemical reaction," *Phys. Fluids* **15**, 3856 (2003).

- <sup>17</sup>S. Subramaniam and S. B. Pope, "A mixing model for turbulent reactive flows based on Euclidean minimum spanning trees," *Combust. Flame* **115**, 487 (1998).
- <sup>18</sup>A. Y. Klimenko, "On simulating scalar transport by mixing between Lagrangian particles," *Phys. Fluids* **19**, 031702 (2007).
- <sup>19</sup>C. Dopazo, "Relaxation of initial probability density functions in the turbulent convection of scalar fields," *Phys. Fluids* **22**, 20 (1979).
- <sup>20</sup>J. Janicka, W. Kolbe, and W. Kollmann, "Closure of the transport equation for the probability density function of turbulent scalar fields," *J. Non-Equilib. Thermodyn.* **4**, 47 (1979).
- <sup>21</sup>S. B. Pope, "Mapping closures for turbulent mixing and reaction," *Theor. Comput. Fluid Dyn.* **2**, 255 (1991).
- <sup>22</sup>H. Chen, S. Chen, and R. H. Kraichnan, "Probability distribution of a stochastically advected scalar field," *Phys. Rev. Lett.* **63**, 2657 (1989).
- <sup>23</sup>J. C. Song, "A velocity-biased turbulent mixing model for passive scalars in homogeneous turbulence," *Phys. Fluids* **30**, 2046 (1987).
- <sup>24</sup>R. O. Fox, "On velocity-conditioned scalar mixing in homogeneous turbulence," *Phys. Fluids* **8**, 2678 (1996).
- <sup>25</sup>A. Y. Klimenko and R. W. Bilger, "Conditional moment closure for turbulent combustion," *Prog. Energy Combust. Sci.* **25**, 595 (1999).
- <sup>26</sup>S. B. Pope, *Turbulent Flows* (Cambridge University Press, Cambridge, England, 2000).
- <sup>27</sup>L. R. SaeTRAN, D. R. Honnery, S. H. Stårner, and R. W. Bilger, *Turbulent Shear Flows 6* (Springer-Verlag, Berlin, 1989), pp. 109–118.
- <sup>28</sup>R. W. Bilger, L. R. SaeTRAN, and L. V. Krishnamoorthy, "Reaction in a scalar mixing layer," *J. Fluid Mech.* **233**, 211 (1991).
- <sup>29</sup>J. D. Li and R. W. Bilger, "Measurement and prediction of the conditional variance in a turbulent reactive-scalar mixing layer," *Phys. Fluids A* **5**, 3255 (1993).
- <sup>30</sup>A. Y. Klimenko, "MMC modelling and fluctuations of the scalar dissipation," in *Proceedings of 2003 Australian Symposium on Combustion and The Eighth Australian Flame Days* (Monash University Printing Services, Clayton, Victoria, 2003), p. P020.
- <sup>31</sup>S. B. Pope, "Accessed compositions in turbulent reactive flows," *Flow, Turbul. Combust.* **72**, 219 (2004).
- <sup>32</sup>J. Villermaux and J.-C. Devillon, "Representation of the coalescence and the redispersion of the fields of segregation in a fluid by a model of phenomenologic interaction," in *Chemical Reaction Engineering: Proceedings of the Fifth European/Second International Symposium on Chemical Reaction Engineering* (Elsevier, New York, 1972), pp. (B1–13)–(B1–24).
- <sup>33</sup>C. Dopazo and E. E. O'Brien, "An approach to the autoignition of a turbulent mixture," *Acta Astronaut.* **1**, 1239 (1974).